J|A|C|S
ARTICLES
Published on Web 10/26/2002

Mesoscopic Monodisperse Ferromagnetic Colloids Enable Magnetically Controlled Photonic Crystals

Xiangling Xu,[†] Sara A. Majetich,[‡] and Sanford A. Asher*,[†]

Contribution from the Department of Chemistry, University of Pittsburgh, Pittsburgh, Pennsylvania 15260 and Department of Physics, Carnegie Mellon University, Pittsburgh, Pennsylvania 15213

Received May 14, 2002

Abstract: We report here the first synthesis of mesoscopic, monodisperse particles which contain nanoscopic inclusions of ferromagnetic cobalt ferrites. These monodisperse ferromagnetic composite particles readily self-assemble into magnetically responsive photonic crystals that efficiently Bragg diffract incident light. Magnetic fields can be used to control the photonic crystal orientation and, thus, the diffracted wavelength. We demonstrate the use of these ferromagnetic particles to fabricate magneto-optical diffracting fluids and magnetically switchable diffracting mirrors.

Introduction

There is intense interest in the nanoscale and mesoscale chemical fabrication of novel photonic crystal materials whose properties can be externally controlled.[1−20] For example, a variety of photonic crystals have been developed which are responsive to their thermal, chemical, and photonic environments.[1−5,19,20] Most recently, we developed the first magnetically controllable photonic crystals[16,17] which were fabricated through the magnetic self-assembly of monodisperse, highly charged, superparamagnetic composite polystyrene colloidal particles; these polystyrene particles contained superparamagnetic iron oxide nanoparticles. We demonstrated a new magnetic field induced crystalline colloidal array (CCA) self-assemble motif based on the attraction of these superparamagnetic particles to the location of magnetic field gradient maxima.

We also formed soft solid polymerized CCA (PCCA) by polymerizing the face-centered cubic (fcc) array of superparamagnetic particles within a hydrogel matrix. Magnetic fields can reversibly deform the superparamagnetic PCCA fcc lattice to shift the Bragg diffraction wavelength. We should note that Gates et al.[18] demonstrated another approach to fabricating superparamagnetic photonic crystals, where monodisperse polystyrene colloids were assembled into a close packed fcc array in an ferrofluid containing nanometer-sized magnetite. The magnetic nanoparticles filled the interstices between the polystyrene particles.

We report here the fabrication of the first monodisperse, mesoscopic ferromagnetic particles. These novel ferromagnetic particles contain nanoscopic inclusions of cobalt ferrite in mesoscopic polystyrene colloids. These ferromagnetic composite particles readily self-assemble into magnetically responsive photonic crystals that efficiently diffract light.

Magnetic fields can control the ferromagnetic photonic crystal orientation and position in space as well as its diffracted wavelength. We demonstrate the use of these materials to fabricate magneto-optical photonic crystal fluids that act as magnetically controlled light modulators. These materials also form magnetically tunable optical switches and mirrors.

Results and Discussion

Synthesis and Characterization of Ferromagnetic Polystyrene Particles. Ferromagnetic composite colloidal particles were synthesized by emulsion polymerization, using methods similar to those used to synthesize our mesoscopic superparamagnetic particles.[16,17] First, ∼20-nm cobalt ferrite particles were formed by coprecipitation of $CoCl_2$ and $FeCl_3$ (mole ratio 1:2) in a 1 M tetramethylammonium hydroxide (TMAOH) solution.[21−24] The XRD measurements shown in Figure 1 indicate that the resulting nanocrystals are in an inverse spinel

* To whom correspondence should be sent. Telephone: (412) 624-8570. Fax: (412) 624−0588. E-mail: asher@pitt.edu.
[†] University of Pittsburgh.
[‡] Carnegie Mellon University.

(1) Asher, S. A.; Holtz, J.; Weissman, J.; Pan, G. *MRS Bull.* **1998**, *23*, 44−50.
(2) Holtz, J. H.; Asher, S. A. *Nature* **1997**, *389*, 829−32.
(3) Weissman, J. M.; Sunkara, H. B.; Tse, A. S.; Asher, S. A. *Science* **1996**, *274*, 959−60.
(4) Pan, G. S.; Kesavanorrthy, R.; Asher, S. A. *Phy. Rev. Lett.* **1997**, *78*, 3860−3.
(5) Tse, A. S.; Wu, Z.; Asher, S. A. *Macromolecules* **1995**, *28*, 6533−8.
(6) Asher, S. A. U.S. Patent 4,627,689 (1986) and 4,632,517 (1986).
(7) Murray, C. B.; Kagan, C. R.; Bawendi, M. G. *Science* **1995**, *270*, 1335−8.
(8) Springholz, G.; Holy, V.; Pinczolits, M.; Bauer, G. *Science* **1998**, *282*, 734−7.
(9) Johnson, S. A.; Ollivier, P. J.; Mallouk, T. E. *Science* **1999**, *283*, 963−5.
(10) Sun, S.; Murray, C. B.; Weller, D.; Folks, D. L.; Moser, A. *Science* **2000**, *287*, 1989−92.
(11) Graf, C.; Blaaderen, A. *Langmuir* **2002**, *18*, 524−34.
(12) Breen, M. L.; Dinsmore, A. D.; Pink, R. H.; Qadri, S. B.; Ratna, B. R. *Langmuir* **2001**, *17*, 903.
(13) Toader, O.; John, S. *Science* **2001**, *292*, 1133−5.
(14) Jiang, P.; Bertone, J. F.; Colvin, V. L. *Science* **2001**, *291*, 453−7.
(15) Muller, M.; Zentel, R.; Maka, T.; Romanov, S. G.; Torres, C. M. S. *Chem. Mater.* **2000**, *12*, 2508−12.
(16) Xu, X.; Friedman, G.; Humfeld, K. D.; Majetich, S. A.; Asher, A. S. *Adv. Mater.* **2001**, *13*, 1681−3.
(17) Xu, X.; Friedman, G.; Humfeld, K. D.; Majetich, S. A.; Asher, A. S. *Chem. Mater.* **2002**, *14*, 1249−56.
(18) Gates, B.; Xia, Y. *Adv. Mater.* **2001**, *13*, 1605−8.
(19) Gu, Z.; Fujishima, A.; Sato, O. *J. Am. Chem. Soc.* **2000**, *122*, 12387−8.
(20) Debord, J. D.; Lyon, L. A. *J. Phys. Chem. B* **2000**, *104*, 6327−31.

10.1021/ja026901k CCC: $22.00

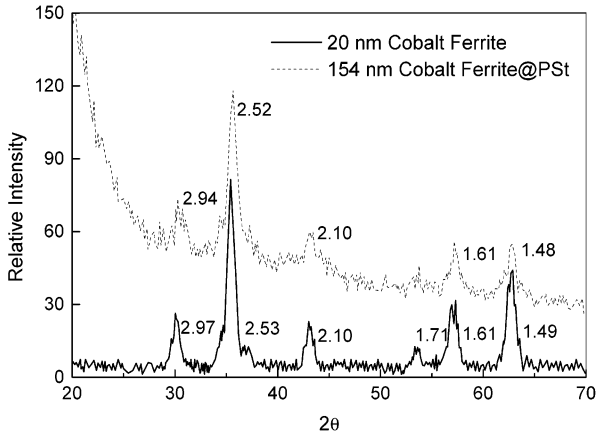

Figure 1. X-ray powder diffraction pattern (Cu Kα radiation) of 20-nm cobalt ferrite and 154-nm polystyrene cobalt ferrite composite particles.

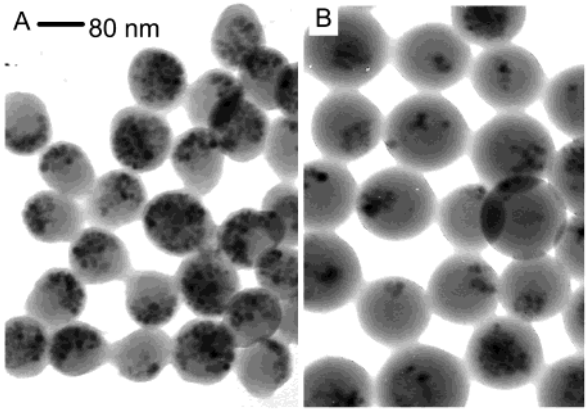

Figure 2. TEM image of ferromagnetic polystyrene composite particles containing cobalt ferrite nanoparticles. (A) TEM image of 120-nm composite particles with a size polydispersity of 7%. The particles contain 14 wt % cobalt ferrite. (B) TEM image of 154-nm composite particles with a size polydispersity of 6%. The particles contain 5 wt % cobalt ferrite. The cobalt ferrite particles appear as black dots inside the composite particles.

structure.[21,25] Since only tiny differences occur between the XRD of Fe_3O_4 and $CoFe_2O_4$, XRD cannot be used directly to determine purity. The cobalt/iron ratio (1:2.2) in the crystal measured by atomic absorption is consistent with pure $CoFe_2O_4$ nanocrystals.

These cobalt ferrite particles were incorporated within polystyrene colloidal particles by emulsion polymerization.[26] The resulting monodisperse ferromagnetic particles were harvested with a magnet (∼10% yield).

We can vary the cobalt ferrite loading in the polystyrene spheres by varying the concentration of cobalt ferrite nanoparticles in the emulsion polymerization reaction. For example, Figure 2 shows the TEM images of ∼120-nm (polydispersity 7%, Figure 2A) and ∼154-nm (polydispersity 6%, Figure 2B) ferromagnetic particles. The nanoscale cobalt ferrite particles

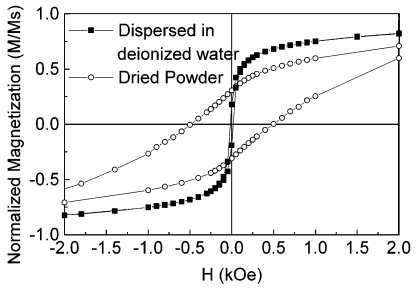

Figure 3. Magnetic behavior of a dried powder and a deionized water dispersion (1.6 wt %) of 120-nm ferromagnetic particles. The magnetization observed was normalized to the saturation magnetization (M_S) observed at 50 kOe. The powder magnetization curve clearly shows hysteresis, while the solution dispersion does not. The larger reduced magnetization (M/M_S) observed for the liquid dispersion presumably results from the ability of these particles to orient with their easy magnetic axes along the field.

appear as black inclusions in TEM images. The cobalt ferrite loading is obviously smaller in the 154-nm (Figure 2B) particles. Although the mesoscopic polystyrene ferromagnetic composite particles are reasonably monodisperse, the TEM indicates significant polydispersity in the cobalt ferrite loading.

We used a SQUID magnetometer to measure the magnetic properties of these particles at room temperature. For a dried powder of the ∼120-nm particles, we observe hysteresis that demonstrates ferromagnetism (Figure 3), a saturation magnetization, M_S, at 50 kOe of 7.2 emu/g (7.0×10^{-15} emu/particle) and a remanent magnetization of 1.7 emu/g (1.6×10^{-15} emu/particle). The remanent magnetization persists indefinitely. For the ∼154-nm particles, we observe a saturation magnetization, M_S, of 2.5 emu/g (4.9×10^{-15} emu/particle) and a remanent magnetization of 0.55 emu/g (1.0×10^{-15} emu/particle). From the 51 emu/g measured saturation magnetization of a powder of our nanoscopic cobalt ferrite particles, we calculate a 14 wt % cobalt ferrite fraction in the 120-nm particles and a 5 wt % cobalt ferrite fraction in 154-nm composite particles.

Magnetically Controlled Orientation of Single Ferromagnetic Particle. Inhomogeneous magnetic fields generate translational forces on all magnetic particles,[27] while homogeneous magnetic fields induce physical torques only on ferromagnetic particles. This torque attempts to rotate the particles to align their magnetic moments along the magnetic field. In contrast, superparamagnetic particles show only Néel rotation, where the magnetic moments of the particles rotate, but not the particles themselves. In a superparamagnet, Néel rotation is rapid relative to the measurement time, but in small ferromagnetic particles, Brownian rotation predominates.[27]

The Figure 3 room temperature hysteresis occurs because the magnetic torque is insufficient to reorient the entire sample and Néel relaxation in the ferromagnet is negligibly slow. In contrast, no hysteresis is observed for these same particles in a 1.6 wt % aqueous dispersion at room temperature (Figure 3) because they rapidly rotate and align with the field within the measurement time. The larger reduced magnetization (M/M_S) observed for the liquid dispersion compared to that of the powder results from the ability of spheres to rotate until their easy magnetic axes lie parallel to the field.

Thus, a strong magnetic field induces a permanent magnetic moment in these particles. A weaker magnetic field can then

(21) Vincente, J.; Delgado, A. V.; Plaza, R. C.; Duran, J. D. G.; Gonzalez-Caballero, E. *Langmuir* **2000**, *16*, 7954−61.
(22) Kang, Y. S.; Risbud, S.; Rabolt, J. F.; Stroeve, P. *Chem. Mater*. **1996**, *8*, 2209−11.
(23) Tang, Z. X.; Sorensen, C. M.; Klabunde, K. J.; Hadjipanayis, G. C. *J. Colloid Interface Sci.* **1991**, *146*, 38−51.
(24) Sauzedde, F.; Elaissari, A.; Pichot, C. *Colloid Polym. Sci.* **1999**, *277*, 846−55.
(25) Rondinone, A. J.; Samia, A. C. S.; Zhang, Z. J. *J. Phys. Chem. B* **1999**, *103*, 6876−80.
(26) Yanase, N.; Noguchi, H.; Asakura, H.; Suzuta, T. *J. Appl. Polym. Sci.* **1993**, *50*, 765−76.
(27) Cullity, B. D. *Introduction to Magnetic Materials*; Addison-Wesley: Reading, MA, 1972.

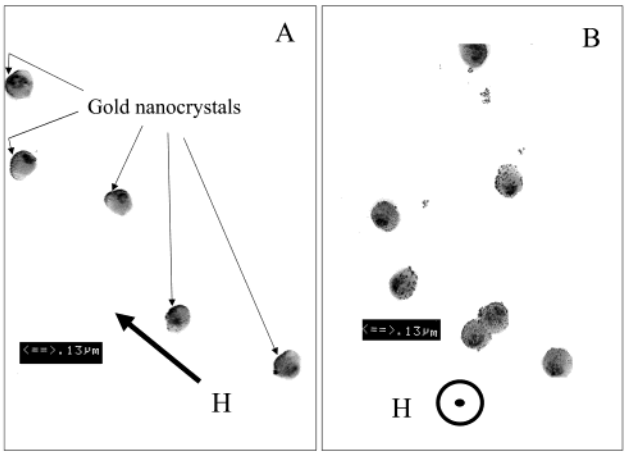

Figure 4. Demonstration of magnetically controlled orientation of magnetized ferromagnetic particles. The magnetized ferromagnetic particles are labeled with a gold patch on their north pole. An aqueous drop containing the magnetized particles was dried onto the TEM grid in the presence of a 300-Oe magnetic field. (A) The magnetic field was oriented as shown within the TEM grid plane. The outward normals to the gold patches orient along the magnetic field direction. (B) The magnetic field was oriented normal to the TEM grid plane, pointed toward the observer. The outward normals to the gold patches point towards the observer.

act on this moment to control the orientation of these ferromagnetic particles. We demonstrated this by coating the ~120-nm ferromagnetic particles with a thin silica shell[28] and then drying these ferromagnetic particles on a substrate. A permanent magnetic moment was induced in these particles by applying a 6-kOe magnetic field normal to the substrate plane. The north pole of each sphere was labeled by sputtering gold onto the exposed north pole surfaces.[29]

These labeled spheres were then redispersed into deionized water, and a drop of this dispersion was dried onto a TEM grid in a homogeneous 300 Oe magnetic field, either oriented within the TEM grid plane or normal to it. TEM measurements of the particles (Figure 4A and B) clearly show that the 300-Oe magnetic field rotates the ferromagnetic particles to orient their magnetic moments along the applied magnetic field. Figure 4A shows that the spheres orient with the outward normals to the gold patches pointing toward the upper left corner, in the direction of the applied field. When the magnetic field is normal to the TEM grid plane, the gold patches orient with their normals toward the observer (Figure 4B).

Fabrication and Response of Ferromagnetic Photonic Crystals to External Magnetic Fields. Our monodisperse ferromagnetic colloidal particles can be induced to magnetically self-assemble into CCA in a manner similar to that demonstrated for superparamagnetic particles.[16,17] This magnetic self-assembly is induced by placing a magnet next to a cell containing magnetic particles; the particles are attracted by the magnetic field divergence and slowly pack into a three-dimensional array against the wall of a container. Because the particles have a large surface charge, they also spontaneously self-assemble into a fcc CCA photonic crystal in low ionic strength aqueous solution, as a result of the strong electrostatic repulsion between neighboring particles. These photonic crystals can be transiently magnetized by a strong magnetic field; the CCA will possess a

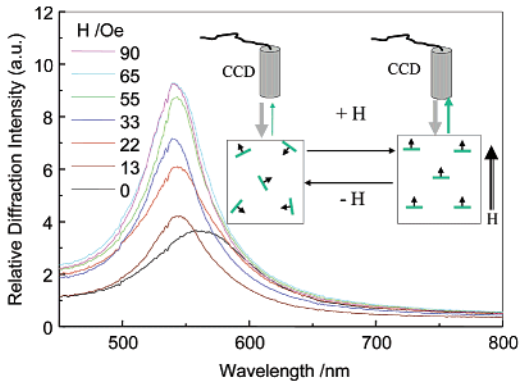

Figure 5. Response of ferromagnetic composite PCCA fragments to an external magnetic field. In the absence of a magnetic field, the fiber optic probe only detects weak back diffraction from the small number of fragments fortuitously oriented with their 111 directions parallel to the fiber optic probe. Application of a magnetic field orients the fragments with their normals along the fiber optic probe, which results in an increased diffraction intensity. The small magnetic field induced diffraction wavelength blue shift occurs because the magnetic field was not exactly parallel to the fiber optic axis.

macroscopic magnetic moment because of the summed contribution of the magnetic moments of the individual ferromagnetic colloidal spheres of the CCA. However, the magnetization quickly dissipates because of the free rotations of the spheres within the CCA.

However, we can create a macroscopically magnetized photonic crystal by polymerizing a CCA of ferromagnetic particles into a hydrogel (PCCA) to lock the position and orientation of these particles relative to one another. We should observe a net magnetization of the ferromagnetic PCCA such that magnetic fields can now be used to control the orientation of this ferromagnetic photonic crystal in order to control the wavelength of light diffracted by the photonic crystal.

For example, we self-assembled ~154-nm monodisperse high surface charged ferromagnetic polystyrene particles (5 wt % cobalt ferrite) into a CCA which we then polymerized into a ~35-μm thick acrylamide hydrogel film.[30] The PCCA fcc 111 plane, which orients parallel to the plane of the PCCA film, has a lattice spacing such that it Bragg diffracts 540-nm normally incident light. We used a 3-kOe magnetic field to magnetize the PCCA such that its magnetic moment was oriented normal to the PCCA film. We then shredded this PCCA into small fragments (~100 μm × ~100 μm × 35 μm). Each PCCA fragment possesses a macroscopic magnetic moment because of the summed contribution of the magnetic moments of the individual ferromagnetic colloidal spheres.

We measured the diffraction from this PCCA film dispersion by using a nine-around-one fiber optic probe. Incident white light from the central fiber is back diffracted by the PCCA fragments and collected by the nine surrounding fibers (Figure 5). In the absence of a magnetic field, we only detect weak diffraction from the small number of fragments fortuitously oriented with their 111 directions almost parallel to the fiber optic probe.[31] Application of a magnetic field orients the fragment normals parallel to the fiber optic probe axis; the diffracted intensity increases with the magnetic field strength.

(28) Tissot, I.; Novat, C.; Lefebvre, F.; Bourgeat-Lami, E. *Macromolecules* **2001**, *34*, 5737−9.
(29) Takei, H.; Shimizu, N. *Langmuir* **1997**, *13*, 1865−8.
(30) Asher, S. A.; Holtz, J.; Liu, L.; Wu, Z. *J. Am. Chem. Soc.* **1994**, *116*, 4997−8.
(31) Reese, C. E.; Baltusavich, M. E.; Keim, J. P.; Asher, S. A. *Anal. Chem.* **2001**, *73*, 5038−42.

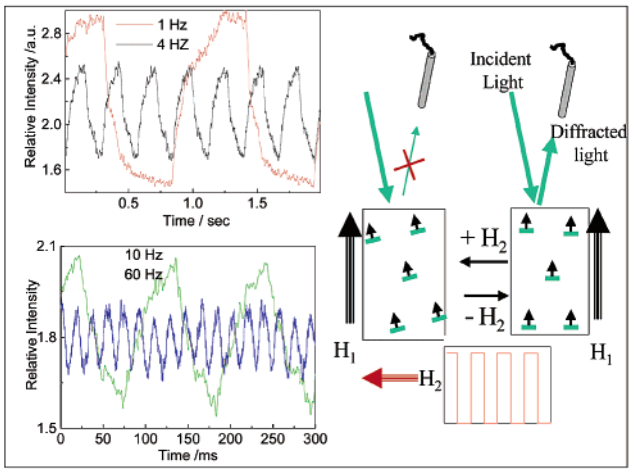

Figure 6. Response of magnetic PCCA to oscillating magnetic field. The PCCA was magnetized with its magnetic moment parallel to the fcc 111 direction, which was normal to the plane of the PCCA film fragments. One electromagnet gave a constant $H_1 = 75$ Oe field along the sample cell normal, while another magnet imposed a perpendicular magnetic field, H_2, which alternated between 0 and 30 Oe. Thus, the net magnetic field orientation oscillates between being normal to the sample cell surface and lying 22° off of the normal. This causes the ferromagnetic PCCA fragment orientation to oscillate and causes an oscillation in diffraction intensity.

Figure 6 shows the response of this magneto-optical fluid to a periodically varying magnetic field. A 543.5-nm He−Ne laser beam was incident as shown, and a fiber optic was oriented such that it collected the diffracted light at a Bragg glancing angle of ∼75°. This diffraction occurs only for those photonic crystals fragments which were oriented such that their normals bisected the angle between the incident and diffracted beam. One electromagnet gave a constant $H_1 = 75$ Oe field along the sample cell normal, while another magnet imposed a perpendicular magnetic field, H_2, which oscillated as a step function between 0 and 30 Oe (Figure 6). This resulted in a net magnetic field direction whose orientation periodically switched between being along the sample cell normal and 22° from the normal. The ferromagnetic photonic crystal fragments reorient in response to the oscillating field which results in an oscillating diffraction intensity (Figure 6).

At the lowest frequencies (<1 Hz), the fragments can fully orient with the field direction within each cycle; thus, a maximum modulation occurs for the diffracted light. At 1 Hz, we observe both a slow and fast rise time within each cycle. These two rise times probably result from a bimodal population of fragment sizes; the smaller fragments completely and promptly orient, while the largest fragments do not have sufficient time to fully orient. Higher frequency modulations (>4 Hz) do not permit fragments to fully orient; thus, the modulation depth of the diffraction decreases (Figure 7).

This dispersion of ferromagnetic photonic crystal fragments acts as a magneto-optical fluid whose diffraction and transmission is controlled by incident magnetic fields. The maximum response rate observed was slightly greater than 70 Hz. This response rate is determined by the reorientation rate, which depends on the magnetically induced torque and the rotational friction. The response rate is expected to dramatically increase as the ferromagnetic photonic crystal fragment size decreases.

We also fabricated a reversible photonic crystal mirror by gluing together two ferromagnetic PCCAs ($2 \times 5 \times 0.2$ mm^3)

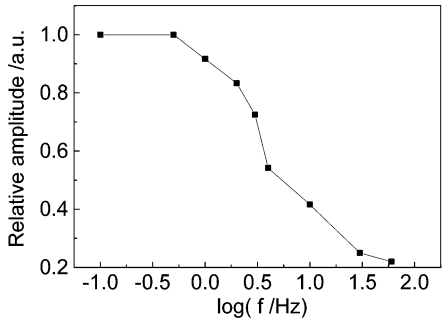

Figure 7. Dependence of the magnetically induced diffraction intensity modulation on the magnetic field switching frequency.

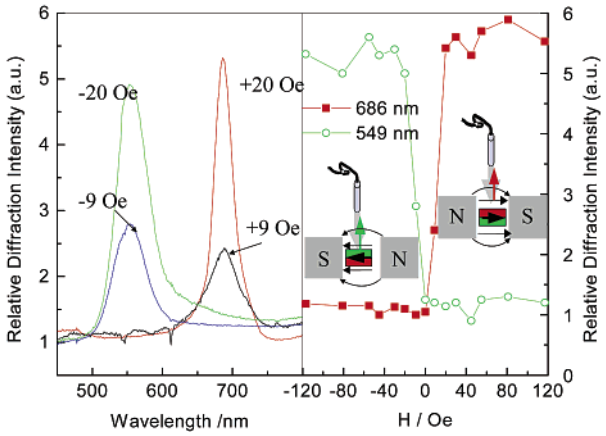

Figure 8. Response of ferromagnetic composite PCCA fragments to an external magnetic field. Two PCCA films with different lattice constants were glued together with their 111 planes parallel to each other. The PCCA magnetic moment was aligned to lie within the 111 plane of the PCCA film. The PCCA film was suspended on a water surface, with the magnetic moment and both PCCA 111 plane normals parallel to the water surface. The figure shows the experimental configuration viewed from the top; the CCD fiber optic probe axis was oriented within the plane of the water surface and normal to the external magnetic field. If the magnetic field points to the left, the PCCA Bragg diffracts ∼549-nm light. If the magnetic field is reversed, the PCCA Bragg diffracts ∼686-nm light.

with different fcc lattice constants. These PCCAs diffract 549- and 686-nm light incident perpendicular to their 111 planes. We then magnetized this photonic crystal laminate with a 3-kOe magnetic field oriented within the PCCA 111 planes. This laminate was sufficiently thick that we were able place this film on the surface of water, with the PCCA 111 plane normal lying parallel to the plane of the water surface. This film could only rotate about an axis normal to the water surface.

Figure 8 shows the magnetic field orientation dependence of this PCCA film diffraction observed by our nine-around-one fiber optic probe, whose axis was oriented within the plane of the water surface and normal to external magnetic field direction. The left panel shows that a magnetic field can control the PCCA film orientation and can switch the surface of the film facing the fiber optic probe. When the magnetic field points to the left, we observe diffraction of 549-nm light. A 180° reversal of the magnetic field rotates the PCCA film such that the other PCCA face diffracts 686-nm light. The diffraction efficiency increases as the field strength increases from 9 to 20 Oe because of the increase in the alignment of the film. This is most clearly shown in the right panel of Figure 8, which shows the dependence of the diffraction wavelength and intensity as a function of the magnetic field strength.

Experimental Section

Synthesis of Cobalt Ferrite Nanoparticles. Nanoscale cobalt ferrite was prepared by the coprecipitation of ferric and cobalt ions in tetramethylammonium hydroxide (TMAOH, Aldrich) solution.[21−24] A 10.8-g amount of $FeCl_3 \cdot 6H_2O$ (J. T. Baker) and 4.8 g of $CoCl_2 \cdot 4H_2O$ (Sigma) were dissolved in 50 mL of water. The resulting solution was poured with vigorous stirring into 500 mL of a 1.0 M TMAOH solution. The resulting brown precipitate was separated by centrifugation. A 500-mL volume of 1 M TMAOH solution was added to the precipitate, and the mixture was sonicated for 1 h. After that, 6.3 g of oleic acid and 1.0 g of sodium dodecyl benzene sulfonate (SDBS, Alcolac) were added to modify the magnetic colloid surface properties.

Synthesis of Ferromagnetic Polymer Particles. Monodisperse ferromagnetic polystyrene cobalt ferrite composite colloidal particles were synthesized by a method similar to that previously used for the synthesis of superparamagnetic particles.[16,17,26] These ferromagnetic particles were synthesized by emulsion polymerization of styrene in the presence of cobalt ferrite, in a jacketed cylindrical reaction vessel that contained a reflux condenser, a Teflon mechanical stirrer, and a nitrogen/reagent inlet. The temperature was maintained through the jacket with the use of a circulating temperature bath. A nitrogen blanket and a stirring rate of 350 rpm were maintained throughout the polymerization.

The reaction vessel containing 180 mL of water and 20 mL of the above cobalt ferrite dispersion was deoxygenated for 30 min. A 30-mL aliquot of styrene (St, Aldrich), 3.0 mL of methyl methacrylate (MMA, Aldrich), and 0.2 g of sodium styrene sulfonate (NaSS, Polyscience) were then added. The temperature was increased to 70 °C, and 2.0 g of APS (ammonium persulfate, Aldrich) was added to initiate the polymerization. The polymerization was carried out for 5 h.

The emulsion polymerization product appeared as dark brown. A magnet was used to harvest the particles containing the cobalt ferrite nanoparticles. We estimate from the magnetization measurements that we magnetically harvested 5% of the polystyrene particles. These polystyrene cobalt ferrite composite particles contain on the average 5 wt % cobalt ferrite nanoparticles. We increased the cobalt ferrite loading by adding more cobalt ferrite particles to the emulsion polymerization recipe. Figure 1A shows ferromagnetic particles containing 14 wt % cobalt ferrite.

Characterization of Nanosize Cobalt Ferrite and Magnetic Composite Particles. X-ray powder diffraction studies utilized a Philips X′PERT system. A Zeiss EM 902A was used to measure the transmission electron micrographs. A Quantum Design MPMS superconducting quantum interference device (SQUID) magnetometer was used to determine the magnetic properties of the cobalt ferrite nanoparticles and the polystyrene cobalt ferrite composite particles at room temperature between ±50 kOe.

PCCA Fabrication. The suspension of polystyrene cobalt ferrite composite particles, which was dialyzed against pure water and then further deionized with ion-exchange resin, self-assembles into a CCA because of the electrostatic repulsion between these highly charged particles. Polymerized CCAs (PCCAs) were prepared by dissolving 0.1 g of acrylamide (Fluka), 0.025 g of cross-linkers *N*,*N*-methylenebisacrylamide (BAM, Fluka), and a drop of UV photoinitiator diethoxyacetophenone (DEAP, Acors) into a 1-mL diffracting suspension containing the polystyrene cobalt ferrite composite particles. This mixture was injected into a cell consisting of two quartz plates, separated by a 35-μm Parafilm spacer. The cell was exposed to UV light from a Blak Ray (365 nm) mercury lamp to initiate polymerization.[30]

Diffraction Measurements. The diffraction spectra of the CCA and PCCA were measured by using a Model 440 CCD UV−vis spectrophotometer (Spectral Instruments, Inc.) coupled to a nine-around-one reflectance probe optical fiber. Incident light transmits out of the central fiber, and we detect the light back diffracted by the CCA collected by the nine surrounding fibers. Transmission measurements were measured by using a Perkin-Elmer Lambda 9 absorption spectrophotometer. The CCA and PCCA samples were always oriented normal to the incident light beam.

Acknowledgment. We thank Dr. Wei Wang and Dr. Chad E. Reese for advice on colloid synthesis. We also thank Prof. Irving Lowe for helpful discussions about magnetism. S.A.A. also acknowledges support for this work from ONR Grant N00014-94-1-0592 and Darpa Contract DAAD16-99-R-1006. S.A.M. acknowledges support from NSF Grant CTS-9800128 and PRF Grant 33866-AC5.

JA026901K